



# Characterization and thermal behavior of $\text{PrMO}_3$ ( $M = \text{Co}$ or $\text{Ni}$ ) ceramic materials obtained from gelatin

F.M. Aquino<sup>a,\*</sup>, D.M.A. Melo<sup>a</sup>, P.M. Pimentel<sup>b</sup>, R.M. Braga<sup>a</sup>, M.A.F. Melo<sup>a</sup>, A.E. Martinelli<sup>a</sup>, A.F. Costa<sup>a</sup>

<sup>a</sup> Federal University of Rio Grande of Norte, Laboratory of Catalysis and Refining – NUPRAR, Av. Senador Salgado Filho, 3000, CEP 59078-970, Natal-RN, Brazil

<sup>b</sup> Universidade Federal Rural do Semi-Árido, Campus Angicos, CEP 59515-000, Angicos-RN, Brazil

## ARTICLE INFO

### Article history:

Received 3 August 2011

Received in revised form 13 April 2012

Accepted 18 April 2012

Available online 25 April 2012

### Keywords:

Ceramic materials

Perovskites

Gelatin

## ABSTRACT

Metal oxides with perovskite-type structure have attracted considerable interest in recent years due to their magnetic and electrical properties, as well as their catalytic activity. In this study, oxides with  $\text{PrNiO}_3$  and  $\text{PrCoO}_3$  composition were prepared by using gelatin powder as a precursor agent for its use as a catalyst. The powders obtained were calcined at 700 °C and 900 °C and characterized using the X-ray diffraction, thermal analysis (thermogravimetry and differential thermal analysis), infrared spectroscopy, temperature programmed reduction and scanning electron microscopy techniques. Thermogravimetric data using the non-isothermal kinetic models of Flynn and Wall and “Model-free Kinetics” were used to determine the activation energy to study the decomposition kinetics of the ligand groups with system's metallic ions that takes part in the synthesis of  $\text{PrMO}_3$  ( $M = \text{Ni}$  or  $\text{Co}$ ).

© 2012 Elsevier Ltd. All rights reserved.

## 1. Introduction

Rare earth cobalt and nickel oxides,  $\text{PrMO}_3$  ( $M = \text{Co}$  or  $\text{Ni}$ ), have been extensively studied due to their interesting electrical and magnetic properties. The  $\text{PrMO}_3$  family, in particular  $\text{Co}$  or  $\text{Ni}$ , provides an interesting window for studying the evolution of the electronic characteristics of the oxides that display metallic conductivity [1–3].

In general, these properties are potentially influenced by the synthesis method, the calcination conditions (temperature, time, and atmosphere) and substitutions of the A and/or B sites. There are several methods for obtaining ceramic oxides with perovskite-type structures. Recent studies make use of gelatin as a polymerization agent and this process appears as a new alternative for obtaining materials with high efficiency and low cost [4].

A preliminary thermogravimetric analysis is sufficient for verifying the temperature at which these oxides are stabilized and the thermal behavior of the material studied. Thermogravimetric analysis (TGA) is one of the most commonly used technologies to study a variety of primary reactions of decomposition of solids and estimate the kinetics parameters of these processes [5].

Thus, a study was conducted on the thermal degradation of organic matter, derived from the gelatin used as a organic precursor in the synthesis of  $\text{PrNiO}_3$  and  $\text{PrCoO}_3$  powders, which

is connected to metal ions in the system, using the kinetic models of Flynn and Wall and “Model free Kinetics”, in order to establish the apparent activation energy as a parameter to characterize and optimize the synthesis conditions for the applicability of the material.

One goal of this work was to synthesize compounds without using high oxygen pressure and long time of calcination. One of the advantages of this method was to produce powders with large amount of porous, with the future goal of their application in catalysis. The method is also a quick and easy route which use low-cost precursor, the gelatin. The disadvantages is the appearance of other phases, but probably disappear if we had increased the calcination time, which would not be interesting, since such materials would be further tested as catalysts and the long time of calcination result in a material with lesser superficial area and fewer porous.

## 2. Experimental

### 2.1. Synthesis of oxide powders

A modified Pechini method was used to synthesize the  $\text{PrNiO}_3$  and  $\text{PrCoO}_3$ . Perovskites were synthesized by using gelatin as a precursor organic and metallic nitrates as starting reagent [5]. Initially, nickel nitrate or cobalt nitrate (Aldrich Chem, 99.9%) was added to a beaker containing deionized water under constant stirring between 60 °C and 70 °C for 5 min. Praseodymium (III) nitrate hexahydrate was added and the system was homogenized for another 5 min. Gelatin was then added to the solution at 70 °C

\* Corresponding author. Tel.: +55 84 3211 9241.

E-mail address: [flavyma@hotmail.com](mailto:flavyma@hotmail.com) (F.M. Aquino).

and stirred for 40 min. Next, the temperature was increased to 90 °C for 1 h, resulting in a resin. After being heat-treated at 350 °C for 2 h, the primary composite oxides were calcined at 700 °C and 900 °C for 4 h.

## 2.2. Materials characterization

The obtained ceramic powders were characterized by various techniques. Infrared absorption spectroscopy (IR) was carried out using KBr pellets. A Shimadzu IR Prestige-21 instrument was used to scan the range of 4500–400  $\text{cm}^{-1}$ . X-ray diffraction was performed using Cu  $K\alpha$  radiation ( $\lambda = 0.15418 \text{ \AA}$ ) in a Shimadzu XRD-6000, the diffraction angles ( $2\theta$ ) were scanned in a range varying between 10° and 90° with a step 0.02° and identification of the compounds were performed by comparison with data from JCPDS – International Center of Diffraction Data. Temperature programmed reduction (TPR) was performed in Micromeritics AUTOCHEM II equipment. The powder with an average weight of 20 mg was heated at a rate of 50  $\text{mL min}^{-1}$ , temperature 30° to 1000 °C, under a gas flow of 10%  $\text{H}_2/\text{Ar}$ . The scanning electron microscopy images were obtained using Philips XL – 30 ESEM equipment, with a power supply of 20 kV. The thermal analysis (TG and DTA) used for the experiments were carried out simultaneously using Shimadzu 60H equipment. Because the Flynn and Wall and “Model-free Kinetics” models require at least three dynamic curves with different heating rates, the following were used: 10, 20 and 30  $^\circ\text{C min}^{-1}$  between room temperature and 700 °C. The mass of the powder was approximately 1 mg, the powder support was alumina, and the carrier gas was synthetic air with a flow of 50  $\text{mL min}^{-1}$ .

## 2.3. Kinetic methods

The ASTM E1641 standard determination of kinetic parameters via thermogravimetry is based on methods proposed by Flynn and Wall [6] and “Model-free Kinetics” [7–9] that are models based on the isoconversion principle, which states that a constant conversion ( $\alpha$ ) of the reaction rate is only a function of temperature, and allow determination of the kinetic parameters of a reaction, as activation energy, by thermal analysis. In the typical experiments is necessary to obtain least at three different heating rates ( $\beta$ ) and plotting  $\ln(\alpha)$  against  $1/T$  giving straight lines with slopes  $-E_\alpha/R$ . The Flynn and Wall kinetic model is an iterative method that uses linear regression to determine the slope and “Model-free Kinetics” is an integral method which allows to evaluate both simple and complex reactions. These methods were used to evaluate which one best fits to determine the apparent activation energy for decomposition gelatin bound to metal ions of the system as a parameter for characterizing and optimizing the conditions of synthesis and applicability of these materials. These models were used to determine the apparent activation energy (Eq. (1)) and conversion ( $\alpha$ ) as a function of temperature.

$$\ln \frac{\beta}{T_\alpha^2} = \ln \left[ \frac{RA}{E_\alpha g(\alpha)} \right] - \frac{E_\alpha}{R} \frac{1}{T_\alpha} \quad (1)$$

Fig. 1 illustrates obtaining the activation energy and pre-exponential factor from the Arrhenius curve (linear regression). As the equation of the line  $y = a_0 + a_1x$  we have, by linear regression fits the best straight line  $y = a_0 + a_1x$ . Thus it have:

$$\alpha_0 = \ln \left[ \frac{RA}{E_\alpha g(\alpha)} \right] e a_1 = \frac{-E_\alpha}{R} \quad (2)$$

From Eq. (2) it possible obtain  $E_\alpha = -R \cdot a_1$ .

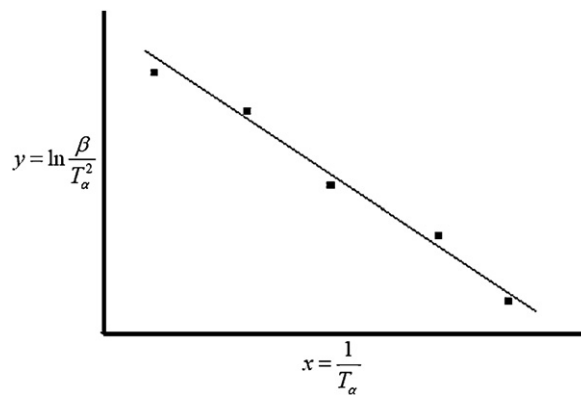


Fig. 1. Curve Arrhenius.

## 3. Results and discussion

The thermogravimetric curves (TG) of the  $\text{PrCoO}_3$  and  $\text{PrNiO}_3$  powders, are represented in Fig. 2. Also in Fig. 2c was observed that the decomposition of the gelatin and the precursor powders occurs in three distinct steps. The first step, which corresponds to a reduction of 12.2%, is associated to humidity (hydration water). The second, around 44.4%, can be attributed to the elimination of amino acid fragments, usually proline, which is thermodynamically susceptible to thermal degradation in oxidant atmosphere. The last step, with mass loss of around 41.4%, may be associated to glycine degradation [10]. Decomposition occurs at higher temperatures for precursor powders, owing to the glycine interaction by means of the carboxylate groups and amine with the metal ions forming the coordination groups, thereby providing more stability to the structure and avoiding the oxidation of a large amount of glycine.

The differential thermal analysis curves of the precursor powders (Fig. 3) show a sharp exothermic peak in the 300–450 °C range. This peak can be attributed to the decomposition processes of the organic groups and the rupture of bonds between the metal ions and carboxyl groups of the organic template [10].

The crystallization of the  $\text{PrCoO}_3$  powder, revealed in Fig. 4, is complete at 700 °C, with the formation of species with  $\text{PrCoO}_3$  perovskite-type structure at a higher proportion and a number of  $\text{Co}_3\text{O}_4$  spinel phase peaks. The results illustrated in Fig. 5 show the diffractograms of the  $\text{PrNiO}_3$  powder, with complete crystallization of  $\text{PrNiO}_3$  structure at 700 °C and isolated oxides such as  $\text{Pr}_6\text{O}_{11}$  and NiO. According to the Escote et al. [11],  $\text{PrNiO}_3$  monophasic

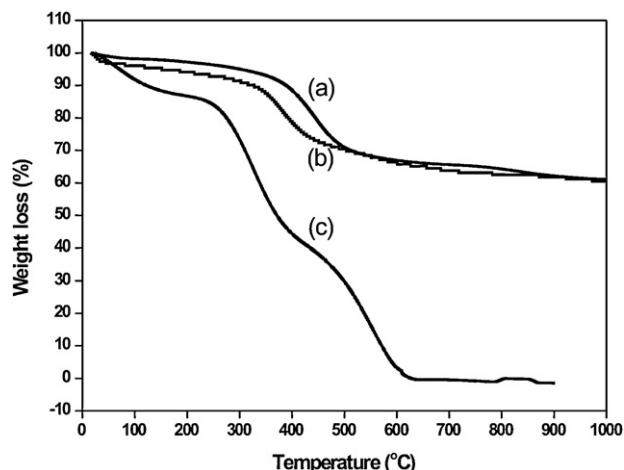


Fig. 2. Thermogravimetric curves of powders (a)  $\text{PrCoO}_3$ , (b)  $\text{PrNiO}_3$  and (c) gelatin.

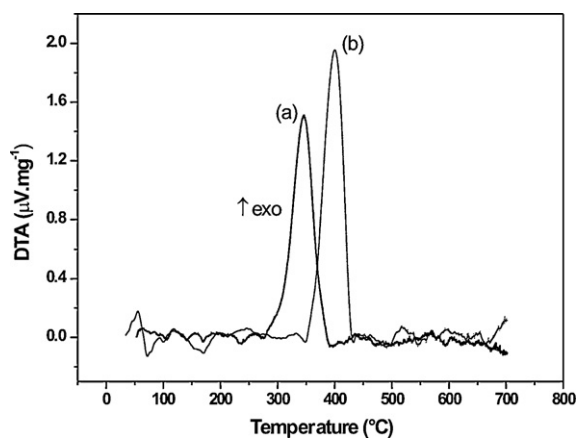


Fig. 3. Differential thermal analysis curves of powders (a) PrCoO<sub>3</sub> and (b) PrNiO<sub>3</sub>.

powders are obtained only from sol-gel methods and high-temperature-high-pressure thermal treatment. Such characteristics suggest that only prolonged thermal treatments under oxygen pressures are capable of eliminating the secondary oxide phases in these materials.

Considering that the phases become crystalline at 700 °C, crystallinity and mean crystallite size were determined. The latter was calculated using the Deybe–Scherrer equation [12,13] (Table 1). According to that, peak width is inversely proportional to mean crystallite size. As expected, crystallinity increased with an increase in calcination temperature, since higher temperatures (greater thermal energy) accelerate the accommodation of atoms in the crystalline structure. Higher temperatures also promote greater crystallite growth.

The absorption spectra in the infrared region for the PrNiO<sub>3</sub> and PrCoO<sub>3</sub> powders treated at 900 °C, respectively are shown in Fig. 6. Characteristic bands can be observed between 600 and 500 cm<sup>-1</sup> in relation to coordination of the cobalt or nickel cation with the carboxylic groups of the gelatin. Spinel structure formation relative to the cobalt oxide (Co<sub>3</sub>O<sub>4</sub>) observed in the X-ray diffractograms for the compound PrCoO<sub>3</sub>. Spinel-type oxides can be seen with two attributions in the FTIR spectrum with frequency  $\nu_1$  of 665 cm<sup>-1</sup> and  $\nu_2$  of 580 cm<sup>-1</sup> [14]. However, to the PrNiO<sub>3</sub> compound was observed bands assigned to ester that is located about 1620 and 1520 cm<sup>-1</sup>, the first peak is assigned to M (C=O), while the second is assigned to M (COO<sup>-</sup>).

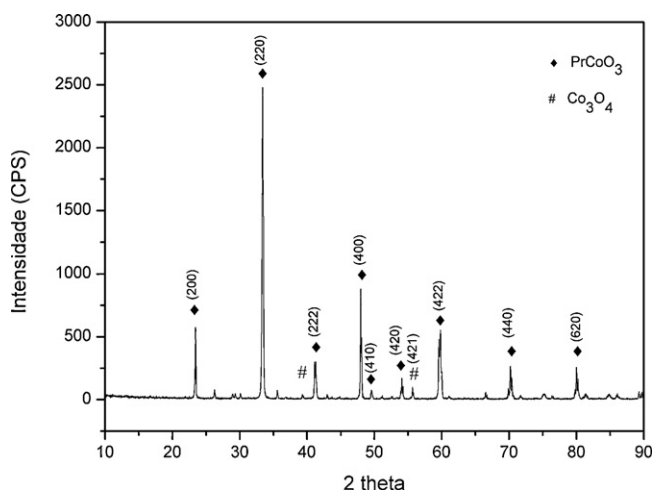


Fig. 4. X-ray diffraction pattern of PrCoO<sub>3</sub> for the powder calcined at 700 °C/ 5 °C min<sup>-1</sup>.

Table 1

Effect of calcination temperature ( $T_{cal}$ ) on crystallinity, crystallite size ( $D_{DRX}$ ) and microdeformations.

	Temperature (°C)	Crystallite size (nm)	Crystallinity (%)
PrCoO <sub>3</sub>	700	44	93
PrCoO <sub>3</sub>	900	83	96
PrNiO <sub>3</sub>	700	48	66
PrNiO <sub>3</sub>	900	52	84

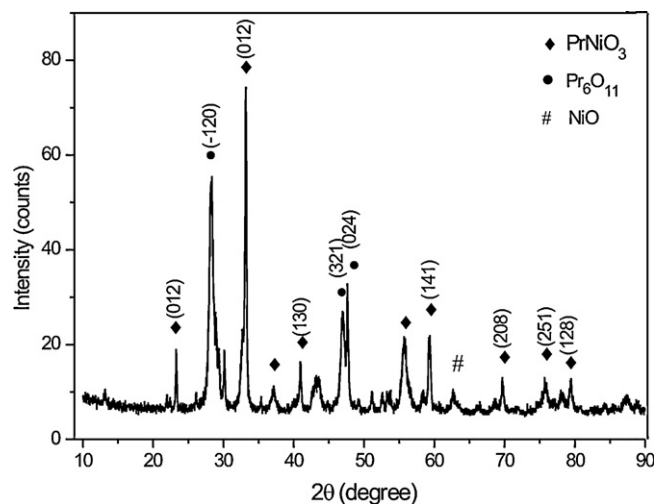


Fig. 5. X-ray diffraction pattern of PrNiO<sub>3</sub> for the powder calcined at 700 °C/ 5 °C min<sup>-1</sup>.

The PrCoO<sub>3</sub> perovskite was reduced in two steps and these two reduction peaks are related to changes in perovskite structure [15,16]. At around 360 °C it is reduced from Co<sup>3+</sup> to Co<sup>2+</sup> and between 510 and 572 °C from Co<sup>2+</sup> to Co<sup>0</sup>. Fig. 7b shows the reduction peaks for the PrCoO<sub>3</sub> powder calcined at 700 °C. They occur at approximately 380 °C relative to the reduction of Co<sup>3+</sup> to Co<sup>2+</sup> and at 514.1 °C relative to the reduction of Co<sup>2+</sup> to Co<sup>0</sup>. The third peak is in lesser proportion, relative to the reduction of the

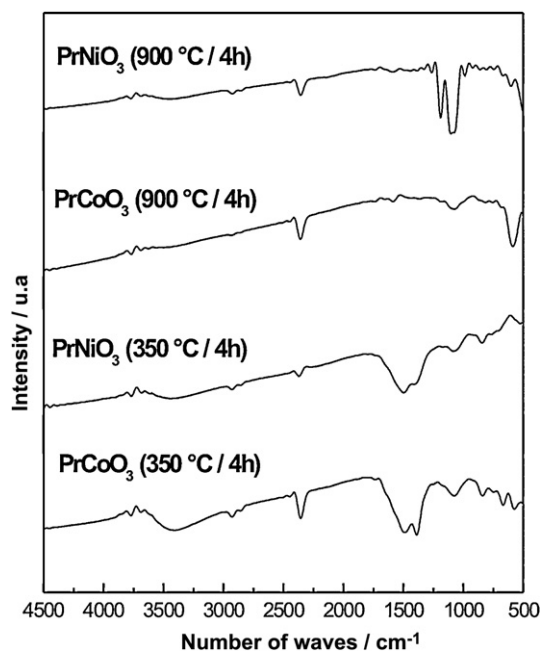


Fig. 6. Absorption spectra in the IR region for the PrNiO<sub>3</sub> and PrCoO<sub>3</sub> powders calcined at 900 °C/4 h.

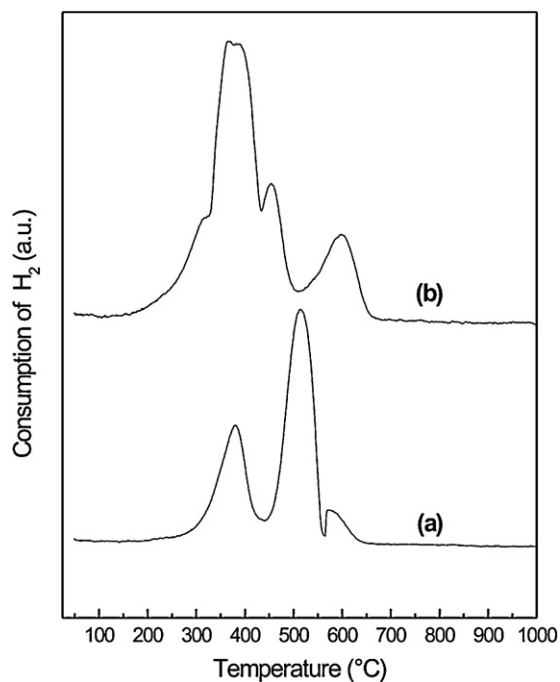


Fig. 7. Profile of temperature programmed reduction for (a) PrCoO<sub>3</sub> and (b) PrNiO<sub>3</sub> calcined at 700 °C/5 °C min<sup>-1</sup>.

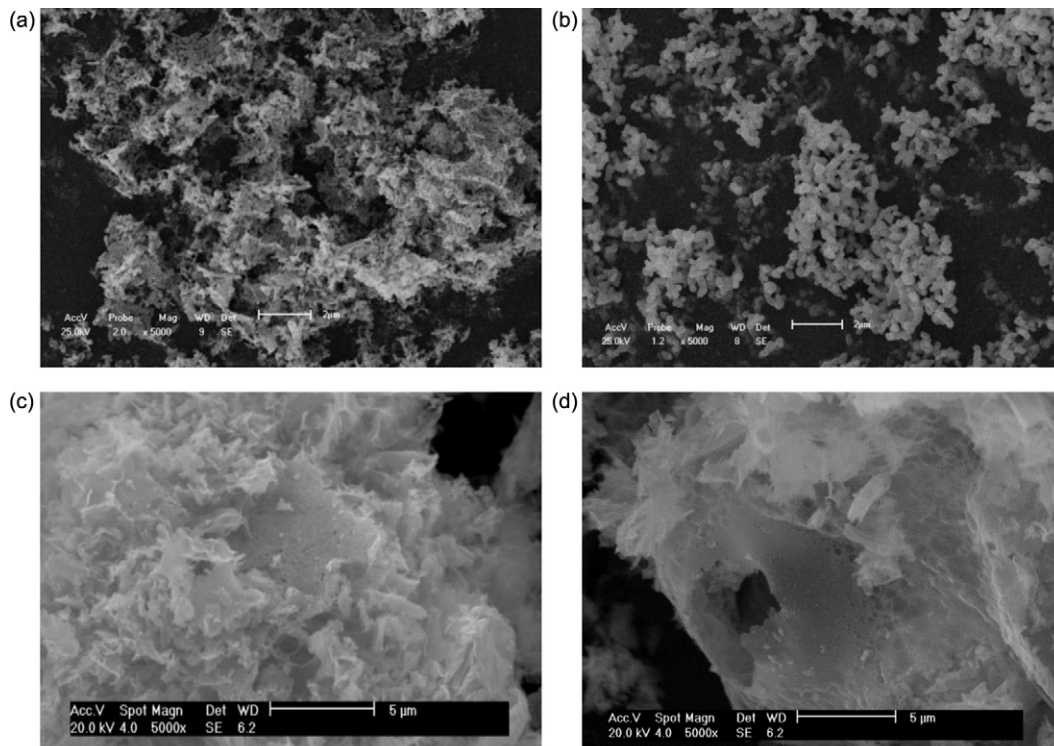
spinel phase at 572.6 °C. The PrNiO<sub>3</sub> peaks of H<sub>2</sub> consumption at 365 °C, 453 °C and 597 °C are also illustrated in Fig. 7a. The first TPR peak corresponds to the first nickel reduction (Ni<sup>3+</sup> → Ni<sup>2+</sup>), while the second peak corresponds to the reduction to metallic nickel

(Ni<sup>2+</sup> → Ni<sup>0</sup>) [17]. The last peak can be attributed to reduction of the segregated NiO phase (Eq. (3)), corroborating previously presented X-ray diffraction results [18].



The micrographs in Fig. 8 show the PrCoO<sub>3</sub> and PrNiO<sub>3</sub> powders calcined at temperatures of (a and c) 700 °C and (b and d) 900 °C, respectively. Fig. 8a and b shows that particles of PrCoO<sub>3</sub> are round with good crystallinity, uniform distribution and little particle agglomeration. Moreover, with an increase in temperature from 700 °C to 900 °C, there is better system organization. The PrNiO<sub>3</sub> powder (Fig. 8c and d) exhibits morphology with considerable porosity and the formation of agglomerated nanometric particles. The gelatin provides the system with a large amount of organic matter, which is then removed during calcinations, favoring the appearance of pores in the material, especially in the nickel powder.

The second and third stages of mass loss obtained from the thermogravimetric curves, above 300 °C, are generally associated to the decomposition processes of organic groups and the breaking of bonds between the metal ions and the carboxyl groups of the gelatin. In these stages were determined the activation energy values involved in process through Flynn and Wall and “Model-free Kinetics” methods. It is observed in Tables 2 and 3 that the values are approximate, with values of linear correlation coefficient near to PrNiO<sub>3</sub> ( $R^2 = 0.97$  for the model of Flynn and Wall and  $R^2 = 0.99$  for Model-free Kinetics) and PrCoO<sub>3</sub> with values of linear correlation coefficient near ( $R^2 = 0.91$  for the model of Flynn and Wall and  $R^2 = 0.98$  for Model-free Kinetics), suggesting that both methods are suitable for the determination of activation energy. However, comparing the activation energy for the compounds and



(a) PrCoO<sub>3</sub> a 700 °C and (b) PrCoO<sub>3</sub> a 900 °C

(c) PrNiO<sub>3</sub> a 700 °C and (d) PrNiO<sub>3</sub> a 900 °C

Fig. 8. Electron micrograph of (a) PrCoO<sub>3</sub> 700 °C; (b) PrCoO<sub>3</sub> 900 °C; (c) PrNiO<sub>3</sub> 700 °C and (d) PrNiO<sub>3</sub> 900 °C.

**Table 2**

Activation energies for the 5.0–90.0% conversions for the PrCoO<sub>3</sub> powders obtained by the Flynn and Wall and “Model-free Kinetics” methods.

Conversion (%)	Model-free Kinetics, $E_a$ (kJ/mol)	Flynn and Wall, $E_a$ (kJ/mol)
5	107	125
10	116	131
20	126	130
30	136	121
40	138	111
50	130	103
60	92	97
70	92	92
80	95	89
90	100	89

**Table 3**

Activation energies for the 5.0–90.0% conversions for the PrNiO<sub>3</sub> powders obtained by the Flynn and Wall and “Model-free Kinetics” methods.

Conversion (%)	Model-free Kinetics, $E_a$ (kJ/mol)	Flynn and Wall, $E_a$ (kJ/mol)
5	153	146
10	156	149
20	147	141
30	130	125
40	115	111
50	105	101
60	96	93
70	89	86
80	83	81
90	77	75

PrCoO<sub>3</sub> and PrNiO<sub>3</sub>, the PrNiO<sub>3</sub> values were slightly higher, which may be due to a higher interaction of the organic matter ligand groups with the metallic ions of the system. What was corroborated by the infrared spectra, because it still possesses carboxyl groups attached to gelatin.

#### 4. Conclusions

The results obtained demonstrate that gelatin, through its carboxylate groups and amine, is an efficient template to be used in the synthesis of ceramic powders, given that it is a chelating and polymerizing agent of metallic ions. With respect to the calcined powders the perovskite phase formation was observed in X-ray diffraction patterns, starting at 700 °C for the two powders studied.

The powders were nanometric and porous. The infrared spectroscopy results obtained reveal characteristic bands between 600 and 500 cm<sup>-1</sup> relative to coordination of the cobalt or nickel cation with the carboxyl groups of the gelatin, for the materials at 700 and 900 °C. Scanning electron microscopy shows that the PrCoO<sub>3</sub> material exhibits round particles, good crystallinity, uniform distribution and no particle agglomeration. For the two powders studied, the activation energy values obtained for the second degradation region with both methods showed a similar behavioral trend, and the values of Pearson correlation coefficients suggest that the studied methods are adequate for determining the kinetic parameter related to decomposition energy, i.e., the interaction of organic matter ligand groups with metallic ions of the system.

#### Acknowledgments

The authors thank to CAPES and CNPq, the Post graduate program in Materials Science and Engineering (PPgCEM) for the financial support and Laboratory of Catalysis and Refining–NUPRAR.

#### References

- [1] D.B. Rogers, J.M. Honigand, J.B. Goodenough, Mater. Res. Bull. 2 (1967) 223–230.
- [2] J.A. Alonso, M.J. Martinez-Lope, I. Rasines, J. Solid State Chem. 120 (1995) 170.
- [3] I.V. Nikulina, M.A. Novojilova, A.R. Kaul, A.F. Maiorovab, S.N. Mudretsovab, Mater. Res. Bull. 39 (2004) 803–810.
- [4] M. Kakihana, J. Sol–Gel Sci. Technol. 6 (1) (1996) 7–55.
- [5] A.O.G. Maia, J. Non-Cryst. Solids 352 (2006) 3729–3733.
- [6] F.S. Oliveira, P.M. Pimentel, R.M.P.B. Oliveira, D.M.A. Melo, M.A.F. Melo, Mater. Lett. 64 (2010) 2700–2703.
- [7] J.H. Flynn, Polym. Lett. 4 (1966) 323–328.
- [8] S. Vyazovkin, C.A. Wight, Thermochim. Acta 340 (1999) 53–68.
- [9] S. Vyazovkin, N. Sbirrazzuoli, Anal. Chim. Acta 355 (1997) 175–780.
- [10] S. Vyazovkin, D. David Dollimore, J. Chem. Inf. Comput. Sci. 36 (1996) 42–45.
- [11] A.S. Menezes, C.M.R. Remédios, J.M. Sasaki, L.R.D. Silva, J.C. Góes, P.M. Jardim, M.A.R. Miranda, J. Non-Cryst. Solids 353 (2007) 1091–1094.
- [12] M.T. Escote, A.M. Silva, J.R. Matos, R.F. Jardim, J. Solid State Chem. 151 (2000) 298–307.
- [13] L.V. Azaroff, Elements of X-Ray Crystallography, McGraw-Hill Book Company, New York, 1968, 552 pp.
- [14] S.F.C.X. Soares. Development of Perovskite Cells for Use Insolid Oxide Fuel, Monograph of Chemistry, Department of Chemistry, University of Rio Grande of Norte, Natal, 2008.
- [15] M.P. Pimentel, A.E. Martinelli, D.M.A. Melo, A.M.G. Pedrosa, J.D. Cunha, C.N. Silva, Mater. Res. 8 (2005) 221–224.
- [16] M.A. Pena, J.L.G. Fierro, Chem. Rev. 101 (2001) 1981–2017.
- [17] R. Lago, J. Catal. 167 (1997) 198–209.
- [18] Y. Eurico, M. Tanabe e Elisabete, Quím. Nova 32 (5) (2009) 1129–1133.